

Effect of Electric Field on Interfacial Thermal Resistance Between Silicon and Water at Nanoscales

Onur Yenigun, Murat Barisik

Department of Mechanical Engineering, Izmir Institute of Technology
35430 Urla, Izmir, Turkey
onuryenigun@iyte.edu.tr; muratbarisik@iyte.edu.tr

Abstract – In this study, heat transfer rate of a nano-confined liquid is controlled by applying an electric field parallel to the heat transfer direction. Molecular Dynamics simulations are performed for deionized water confined between silicon slabs, where their surfaces oppositely charged to create an electric field perpendicular to the silicon wall to promote the electrowetting. Electric field strengths used in this study are 0, 0.18 and 0.35 V/nm. To investigate the effect of electric field on heat transfer, first water density profiles near the silicon walls are examined. Results shows that by applying electric field, water molecules near the silicon walls develop layering, which indicates the increased solid/liquid coupling. With the increasing electric field strength, an increase in the peak of the density layering is observed. Furthermore, heat transfer at the solid/liquid interface is characterized with the Kapitza length values. The results show that applying electric field reduces the interfacial thermal resistance between water and silicon due to the increased solid/liquid coupling and doubles the total heat flux.

Keywords: Electrowetting, Interfacial Thermal Resistance, Kapitza Length, Molecular Dynamics.

1. Introduction

Thermal management of the micro/nano-electromechanical systems (NEMS/MEMS) is still one of the main challenge for the further developments in the field [1]. Decrease of component sizes in micro/nano systems increases the number of interfaces and their influences. At the interface of two dissimilar materials an interfacial thermal resistance (ITR) occurs due to the mismatch of the phonon spectrums. Consequently, ITR becomes the most dominant heat transfer mechanism at nanoscale by the increase of surface-to-volume ratio. The key to overcome the heat dissipation problems of the micro/nano devices is to understand and manipulate the interaction effects at the interfaces.

There are many experimental, theoretical, and computational studies regarding increasing the heat transfer rate by lowering the ITR depending on different molecular properties such as, liquid pressure, surface density, surface temperature, nano-film thickness and surface wetting [2-13]. Even though there are different ways to reduce interfacial thermal resistance, its dependency on solid/liquid coupling (i.e., surface wetting) is investigated by many researchers and proved to be the most effective parameter. Increased wetting ability effects the solid/liquid coupling at the interface by creating liquid layering around the surface at nano-scale [14]. Due to the increased coupling, the heat transfer rate is enhanced as well by the decrease of the interfacial thermal resistance (ITR). In the literature, various methods are applied in order alter the surface wetting, such as; employing nano-structures at the surface [15, 16] or using surface coatings [17, 18]. Despite the fact that these methods are effective, to employ them, the surface morphology should be changed chemically or mechanically. However, surface wetting can be manipulated by applying electric field to the confined liquid, which is known as electrowetting [19, 20]. In this study, effect of various electric field strengths on ITR is investigated by examining liquid temperature and density profiles, Kapitza length and total heat flux.

2. Simulation Details

We employed non-equilibrium molecular dynamics (NEMD) simulations. Simulation domain consists of water confined between two silicon walls as illustrated in Figure 1. Simulations are performed with LAMMPS (Large-scale Atomic/Molecular Massively Parallel Simulator) package for deionized water confined between silicon slabs, where slabs are oppositely charged to create an electric field parallel to the heat transfer direction. Cross sectional area of the computational domain was 3.8×3.8 nm in the vertical and lateral directions, where periodic boundary conditions were

applied. In the longitudinal direction, length of the silicon slabs was 5.4nm while (0, 0, 1) crystal plane was facing the fluid, where channel height was 5.7nm.

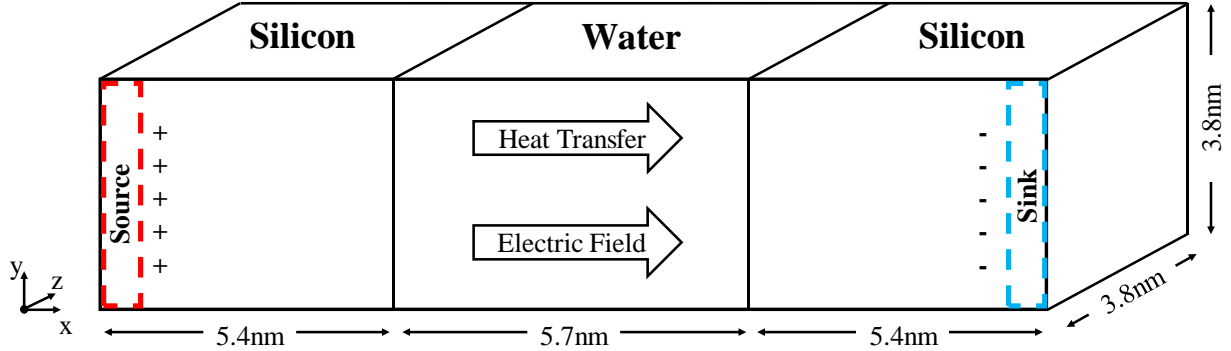


Fig. 1: Schematic of the simulation domain.

Water density was kept at 0.996 g/cm³. SPC/E water model composed of Lennard-Jones and Coulombic potentials is used [21] with SHAKE algorithm to constrain the bond lengths and angles of this rigid model. Stillinger-Weber potential is used for the Si-Si interactions, which considers two-body interactions with an additional many body dependence [22]. The molecular interaction parameters for each molecule pair used in the simulations are given in Table 1. Furthermore, silicon surface charge densities used in this study are 0, 0.11 and 0.22 C/m², which resulted in electric fields of 0, 0.18 and 0.35 V/nm. Atoms in the outmost layer of both Silicon walls are fixed to their original locations to maintain a fixed volume system, while the remaining atoms throughout the domain were free to move. A particle-particle particle-mesh (PPPM) solver which can handle long-range Coulombic interactions for periodic systems with slab geometry is used. Nose Hoover thermostat is applied only on the outmost six layers of the both silicon slabs to induce heat flux through the liquid/solid interfaces by maintaining wall temperatures of 363K and 283K, as source and sink respectively. At the same time, NVE ensemble is applied to the remaining silicon and water molecules. Simulations are performed for 12×10⁶ time-steps to ensure that the system attains equilibrium in presence of the heat flux and time averaging is performed after the equilibrium is achieved. The computational domain is divided into 1476 slab bins with the size of 0.0113nm to resolve the fine details of the water density distributions.

Table 1: Molecular interaction parameters used in the current study.

Molecule Pair	σ (Å)	ϵ (eV)	q (e)
O-O	3.166	0.006739	-0.8476
H-H	0	0	+0.4238
Si-Si	2.095	2.168201	Varies
Si-O	2.6305	0.01511	-

3. Results

Uniform surface charges are introduced to the silicon layers at the water interfaces. Positive charge is applied on the left wall, representing anode and negative charge is applied on the right wall, representing cathode. Under these conditions, an electric field is created in the system from left to right. Temperature of the silicon walls are kept constant at 363K and 283K, as source and sink, respectively. In Figure 2, normalized temperature distributions of water molecules under electric field strengths of 0, 0.18 and 0.35 V/nm are documented. The slope of the temperature profile of water molecules tends to increase with the increasing electric field strength. Since the wall temperatures are the same, we need to take a look at the density profiles varying with the electric field strengths in order to explain the increase in the heat transfer.

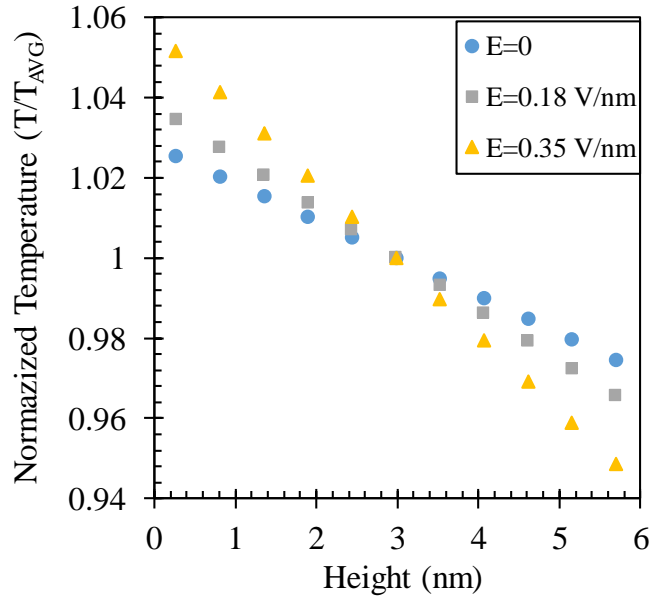


Fig. 2: Normalized temperature profiles of water molecules under varying electric field strengths.

In Figure 3, density distributions of water molecules under electric field strengths of 0, 0.18 and 0.35 V/nm are documented. In all cases, water density reaches its bulk value of 0.996 g/cm³. Increasing density layering as a function of wetting, which is promoted with increasing electric field exposure is observed. Such behaviour is expected, since promoting wetting with applying electric field is a well-known subject as electro-wetting [19, 20]. However, under oppositely charged walls, hydrogen molecules will turn and attracted towards cathode and oxygen molecules towards anode. For this reason, there is a non-symmetrical density distribution developed in the confined water. With increasing electric field strength, water molecules near the walls develop up to three density layers in both walls. The nearest density peak increases by the increase of electric field strength. These increasing density layers indicate that the increased molecular coupling at the interface.

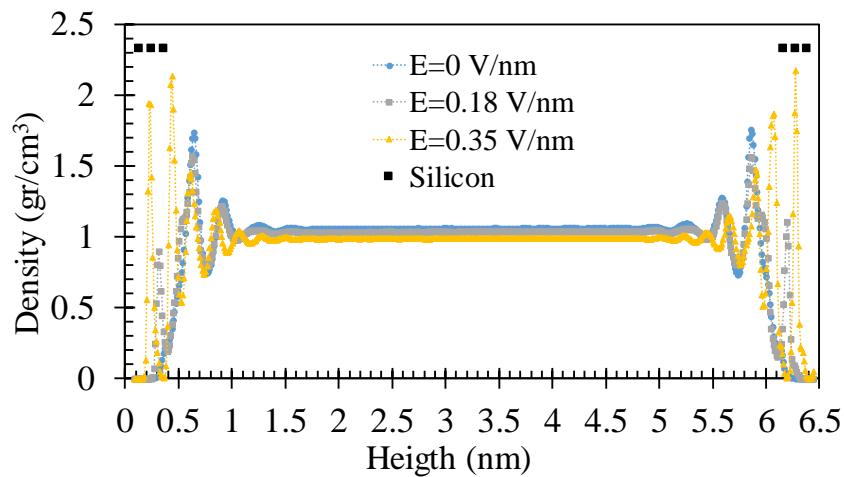


Fig. 3: Density profiles of water molecules under varying electric field strengths.

In Figure 4, variation of Kapitza Length and total heat flux with electric field strength is documented. Kapitza Length, L_K (Equation 1) is the representation of the interfacial thermal resistance between silicon and water, where ΔT is the temperature jump at the liquid/solid interface and $\partial T/\partial n$ is the temperature gradient of the liquid.

$$\Delta T = L_K (\partial T / \partial n) |_{\text{liquid}}, \quad (1)$$

Measured Kapitza Length values for shows that applying electric field can reduce the interfacial thermal resistance between silicon significantly. Interface thermal resistance is decreasing with the increase of electric field strength, because it promotes surface wetting. The increase in water density layering near the silicon walls by the increase in electric field documented in Figure 3, strengthens the solid/liquid coupling at the interface, thus decreases the interfacial thermal resistance. This drop in the interface thermal resistance increases the total heat flux to twice of its original value as shown in Figure 4. Furthermore, to measure the accuracy of the results, a statistical investigation on the L_K values is performed. First, from the total simulation time of 12ns, different time averages obtained at every 2ns, 4ns, 6ns and 12ns. From these time averages, 12 different data sets are obtained and L_K values for each set is calculated. Finally, the standard deviation of L_K is calculated and documented in Fig.4 as error bars around the mean L_K values.

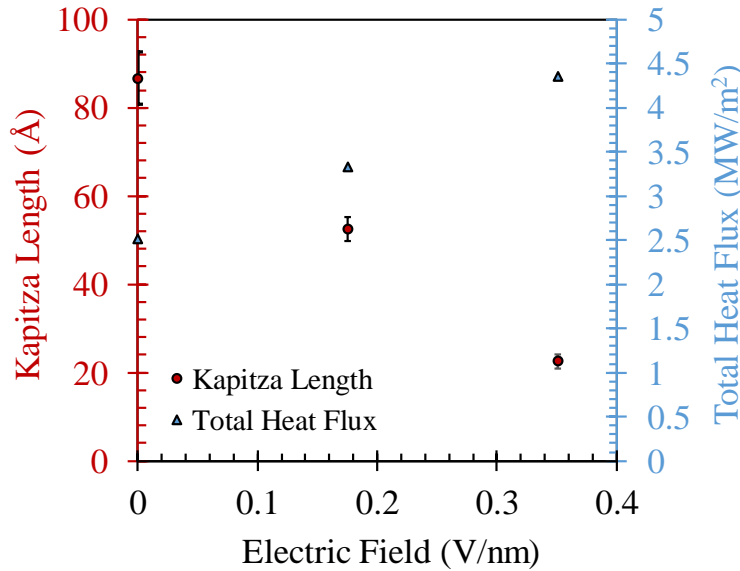


Fig. 4: Kapitza length and total heat flux variation with electric field strength.

4. Conclusion

Molecular Dynamics simulations are performed in order to reveal how interfacial thermal resistance is effected by the applied electric field to a nano confined liquid. The increased slopes of the temperature profiles of water molecules under increasing electric field strengths indicate that the heat transfer rate is increased. To explain this heat transfer enhancement, density profiles of water molecules are investigated. Evolution of the water density layers are observed with the increased electric field strength. These density layers are the proof of enhanced solid/liquid coupling, thus enhanced surface wetting. Furthermore, it is observed that increased solid/liquid coupling at the interface decreases the interfacial thermal resistance and improves the heat transfer rate. To characterize the heat transfer at the interface, Kapitza Length values are measured and a significant decrease in the Kapitza Length is observed. Finally, as a result of applied electric field solid/liquid coupling at the interface is increased and total heat flux is nearly doubled its original value. The results of this study are important for designing micro/nano devices which requires advanced heat removal.

Acknowledgements

Murat Barisik would like to thank Turkish Academy of Sciences (TUBA) in the framework of the Young Scientist Award Programme (GEBIP) for support.

References

- [1] S. V. Garimella, A. S. Fleischer, J. Y. Murthy, A. Keshavarzi, R. Prasher, C. Patel,... & B. Sammakia, "Thermal challenges in next-generation electronic systems," *IEEE Transactions on Components and Packaging Technologies*, vol. 31, no. 4, pp. 801-815, 2008.
- [2] L. Xue, P. Keblinski, S. R. Phillpot, S. S. Choi, & J. A. Eastman, "Effect of liquid layering at the liquid–solid interface on thermal transport," *International Journal of Heat and Mass Transfer*, vol. 47, no. 19-20, pp. 4277-4284, 2004.
- [3] S. Murad & I. K. Puri, "Molecular simulation of thermal transport across hydrophilic interfaces," *Chemical Physics Letters*, vol. 467, no. 1-3, pp. 110-113, 2008.
- [4] M. Barisik & A. Beskok, "Temperature dependence of thermal resistance at the water/silicon interface," *International Journal of Thermal Sciences*, vol. 77, pp. 47-54, 2014.
- [5] O. Yenigun, M. Barisik, "Effect of nano-film thickness on thermal resistance at water silicon interface," *International Journal of Heat and Mass Transfer*, vol. 134, pp. 634-640, 2019.
- [6] Z. Ge, D. G. Cahill, & P. V. Braun, "Thermal conductance of hydrophilic and hydrophobic interfaces," *Physical review letters*, vol. 96, no. 18, p. 186101, 2006.
- [7] B. H. Kim, A. Beskok, & T. Cagin, "Thermal interactions in nanoscale fluid flow: molecular dynamics simulations with solid–liquid interfaces," *Microfluidics and Nanofluidics*, vol. 5, no. 4, pp. 551-559, 2008.
- [8] M. Barisik & A. Beskok, "Boundary treatment effects on molecular dynamics simulations of interface thermal resistance," *Journal of Computational Physics*, vol. 231, no. 23, pp. 7881-7892, 2012.
- [9] A. T. Pham, M. Barisik, & B. Kim, "Interfacial thermal resistance between the graphene-coated copper and liquid water," *International Journal of Heat and Mass Transfer*, vol. 97, pp. 422-431, 2016.
- [10] Z. Shi, M. Barisik, & A. Beskok, "Molecular dynamics modeling of thermal resistance at argon-graphite and argon-silver interfaces," *International Journal of Thermal Sciences*, vol. 59, pp. 29-37, 2012.
- [11] A. T. Pham, M. Barisik, & B. Kim, "Molecular dynamics simulations of Kapitza length for argon-silicon and water-silicon interfaces," *International journal of precision engineering and manufacturing*, vol. 15, no. 2, pp. 323-329, 2014.
- [12] T. Q. Vo, M. Barisik, & B. Kim, "Atomic density effects on temperature characteristics and thermal transport at grain boundaries through a proper bin size selection," *The Journal of chemical physics*, vol. 144, no. 19, pp. 194707, 2016.
- [13] A. Pham, M. Barisik, & B. Kim, "Pressure dependence of Kapitza resistance at gold/water and silicon/water interfaces," *The Journal of chemical physics*, vol. 139, no. 24, p. 244702, 2013.
- [14] M. Barisik, & A. Beskok, "Wetting characterisation of silicon (1, 0, 0) surface," *Molecular Simulation*, vol. 39, no. 9, pp. 700-709, 2013.
- [15] S. Chen, J. Wang, T. Ma, & D. Chen, "Molecular dynamics simulations of wetting behavior of water droplets on polytetrafluorethylene surfaces," *The Journal of chemical physics*, vol. 140, no. 11, p. 114704, 2014.
- [16] T. W. Kwon, J. Jang, M. S. Ambrosia, & M. Y. Ha, "Molecular dynamics study on the hydrophobicity of a surface patterned with hierarchical nanotextures," *Colloids and Surfaces A: Physicochemical and Engineering Aspects*, vol. 559, pp. 209-217, 2018.
- [17] A. R. Motezakker, A. K. Sadaghiani, Y. Akkoc, S. S. Parapari, D. Gözüaçık, & A. Koşar, "Surface modifications for phase change cooling applications via crenarchaeon *Sulfolobus solfataricus* P2 bio-coatings," *Scientific reports*, vol. 7, no. 1, pp. 17891, 2017.
- [18] J. Li, L. Zhou, N. Yang, C. Gao, & Y. Zheng, "Robust superhydrophobic coatings with micro-and nano-composite morphology," *RSC Advances*, vol. 7, no. 70, pp. 44234-44238, 2017.
- [19] F. Mugele & J. C. Baret, "Electrowetting: from basics to applications," *Journal of physics: condensed matter*, vol. 17, no. 28, R705, 2005.
- [20] L. Chen, & E. Bonaccorso, "Electrowetting—From statics to dynamics," *Advances in colloid and interface science*, vol. 210, pp. 2-12, 2014.
- [21] H. J. C. Berendsen, J. R. Grigera, & T. P. Straatsma, "The missing term in effective pair potentials," *Journal of Physical Chemistry*, vol. 91, no. 24, pp. 6269-6271, 1987.
- [22] F. H. Stillinger, & T. A. Weber, "Computer simulation of local order in condensed phases of silicon," *Physical review B*, vol. 31, no. 8, p. 5262, 1985.